8th Pan American Conference for Nondestructive Testing 2025, 9-12.June, 2025 Niagara Falls, Canada

e-Journal of Nondestructive Testing - ISSN 1435-4934 - www.ndt.net

Evaluation of opal photonic crystal films for application in non-destructive testing

Eli Simova [(1)], Krassimir Stoev [(1)], Hiroshi Fudouzi [(2)]

[(1)] Canadian Nuclear Laboratories, Chalk River, Ontario K0J 1J0, Canada
Phone: +1-613-584-3311, e-mail: krassimir.stoev@cnl.ca, eli.simova@cnl.ca
[(2)] National Institute for Materials Science, 1-2-1 Sengen, Tsukuba 305-0031, Japan, fudouzi.hiroshi@nims.go.jp

Abstract
Opal photonic crystal films are based on closely-packed colloidal crystals deposited as thin layers on flexible plastic sheets. They can be used as simple and low-cost devices for visualising deformation, strain, cracks, defects, etc. Such opal photonic films were developed and manufactured at the National Institute for Materials Science (NIMS), Japan, and samples were provided to Canadian Nuclear Laboratories (CNL) for evaluation. Properties of the opal photonic films, together with some approaches for using these devices for non-destructive testing (NDT) of concrete, will be presented and discussed.

Keywords: NDT, opal photonic films, colloidal photonic crystals.

1. Introduction

Opal photonic crystal films (also called photonic sheets) are based on closely-packed colloidal crystals with three-dimensionally periodic lattices, deposited as thin layers on flexible plastic sheets. The films can be used as simple and low-cost devices for visualising deformations, strain, cracks, defects, temperature changes, etc. When photonic sheets are stretched, the change in the spacing of the colloidal particles in the opal film alters the colour of the film. Such opal photonic films were developed and manufactured [1]-[8] at the National Institute for Materials Science (NIMS), Japan. Samples of the photonic sheets were provided to Canadian Nuclear Laboratories (CNL) for evaluation. The following testing activities were carried out at CNL:

- Evaluation of the strain visualising and measuring capabilities of the photonic sheets.
- Study the behaviour of the photonic sheets attached to concrete walls during temperature and load changes.
- Development of methods for non-contact (i.e., stand-off distances of greater than 1 m) quantitative measurement of the photonic sheets.

Some of the results of the tests are presented in this paper.

2. Experimental Setup

Several samples of photonic sheets were provided by NIMS to CNL. One of the samples had 50 µm thickness of the substrate, while the other samples had 100 µm thickness of the substrate. In all cases, the substrate on which the colloidal crystal films were coated, was black colour polyethylene terephthalate (PET) sheet. The samples tested are summarized in Table 1. When viewed from different angles, the photonic sheets change colour from red to green, as the viewing angle increases, as shown in Figure 1. There is a peak in the reflectivity spectrum of the photonic sheet in the range from 550 nm to 650 nm, and this peak is designated as the red peak.

Two types of illumination were used during the experiments: (i) a high brightness phosphor-converted white-light light-emitting diode (LED) panel; and (ii) ambient fluorescent room

 https://doi.org/10.58286/31515

lighting. Two different illuminations were used to assess the need for specialized lighting when using the photonic sheets. The angles of illumination and observation were also adjusted to be close to the optimal angle, between 10 and 14 degrees, which was determined experimentally. The spectra of the LED panel and the fluorescent ambient light are presented in Figure 2. The blue peak (at ~ 445 nm) in the LED spectrum corresponds to blue emission line of the LED semiconductor element, which illuminates the phosphor material used in LED lens, and the phosphor emits yellow light having a broad spectral power distribution from 480 nm to 680 nm.

Table 1: List of photonic sheet samples

Sample Code	PET sheet Thickness [µm]
VH133	100
VH137	50
D100-18	100
D100-19	100
D100-22	100
D100-23	100
D100-24	100

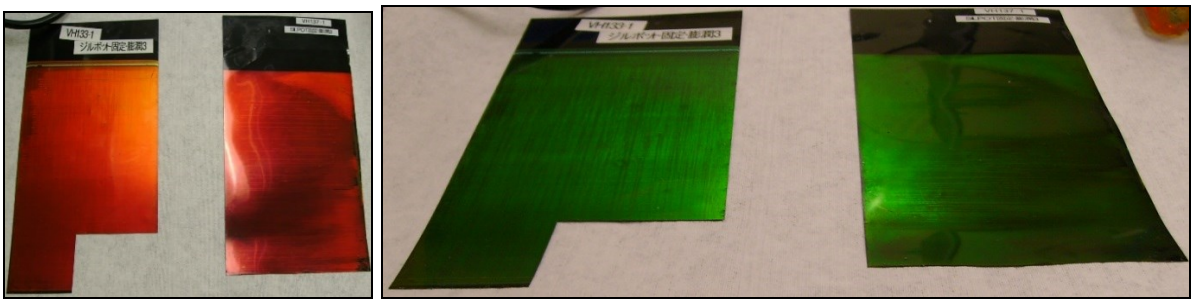

Figure 1: Different viewing angle results in different colour reflected by the photonic sheet.

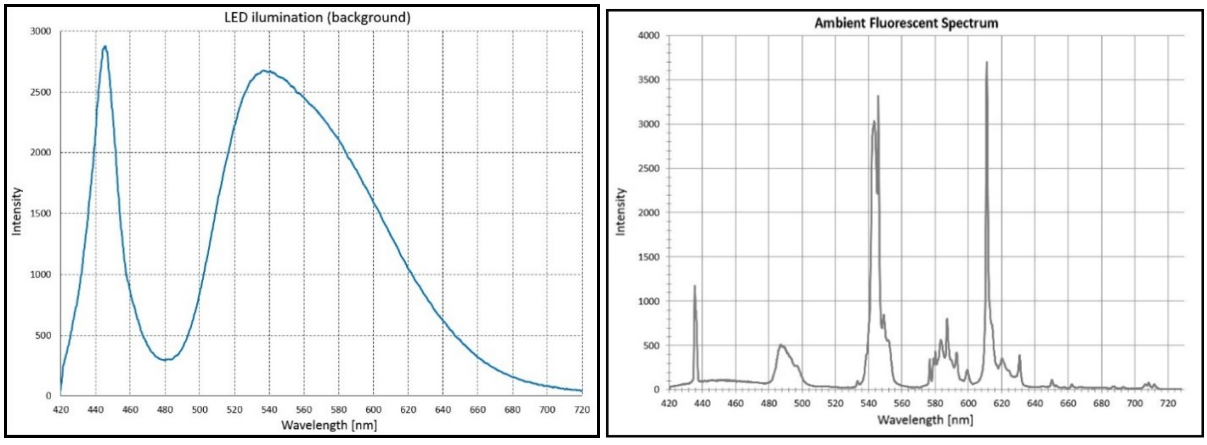

Figure 2: Spectra of LED panel (left) and ambient fluorescent lighting (right).

For the experiment, small portions (strips) of the photonic sheets were cut and used. Some of them were attached to a stretching jig, while the other were glued to concrete blocks. The reflectivity spectra from the photonic sheets were collected with an Ocean Optics USB2000 fibre optics spectrometer. Two measurement setups were prepared: (i) with a fiber optic tip was attached to a vertical rotation stage, which allowed for collecting spectra at different

reflection angles in respect to the surface of the photonic sheet during the stretching experiments, and (ii) a compact handheld holder, which housed the illumination LED and the fibre-optic tip of the spectrometer at a fixed angle of illumination and observation. Examples of the fibre optic measurement setups are presented in Figure 3.

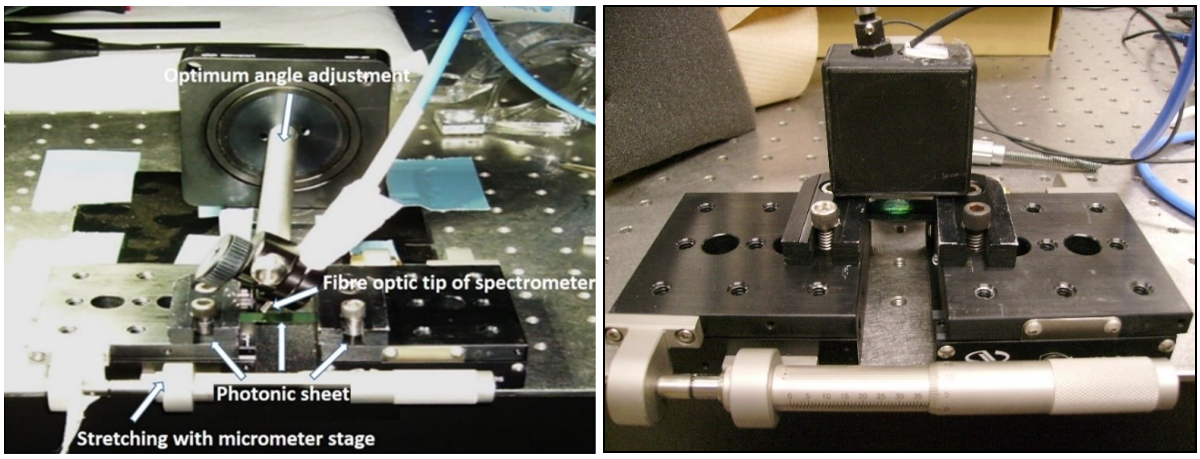

Figure 3: Variable-angle rotation stage (left) and handheld fixed-angle holder (right) setups.

Additional experiments were performed using the same stretching setup with the images recorded with a high-resolution 10 megapixels colour camera from IDS Imaging Inc. The colour camera experiment setup is shown in Figure 4.

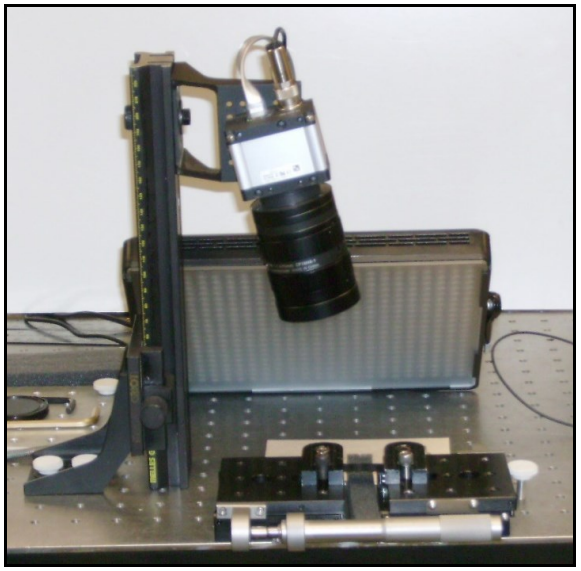
Figure 4: Setup for measurements with high-resolution colour camera.

3. Evaluation of photonic sheets

The following testing activities were carried out at CNL:

- Evaluation of the strain visualising and measuring capabilities of the photonic sheets
- Evaluation of photonic sheets attached to a concrete block during temperature and load changes
- Development of methods for non-contact (i.e., stand-off distance of greater than 1 m) quantitative measurement of the photonic sheets

The results from the tests are presented below in Section 3.

3.1 Spectral response to stretching

For the stretching experiments, a 60 x 10 mm strips from the photonic sheets were clamped to two stages with micrometer control, as shown in Figure 5. This allowed the photonic sheets to be positioned horizontally without bending or wrinkles, and to be stretched with precise control.

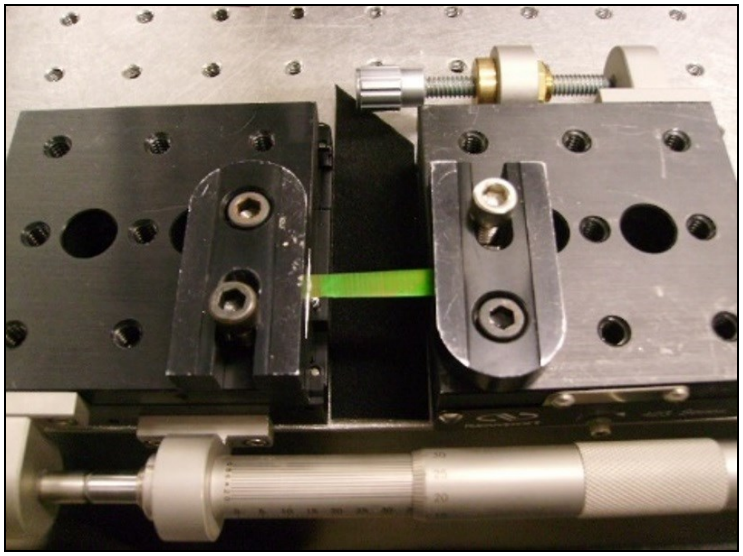

Figure 5: Photonic sheet clamped between two stages with micrometer control.

Reflectivity spectra were collected with the fibre optic spectrometer at different elongations of the sample strips. In order to characterize the source reflection spectrum, the background reflectivity spectrum of a grey neutral sample illuminated with the LED was collected and was used as a reference background spectrum. This background spectrum was subtracted from the raw reflectivity spectra of the photonics sheets to produce a resulting spectrum of the net reflectivity of the opal photonic crystal film. Examples of the raw photonics sheet spectrum, background spectrum and net reflectivity spectrum form a photonics sheet are presented in Figure 6. The spectrum oscillations due to the diffraction effects can be clearly observed.

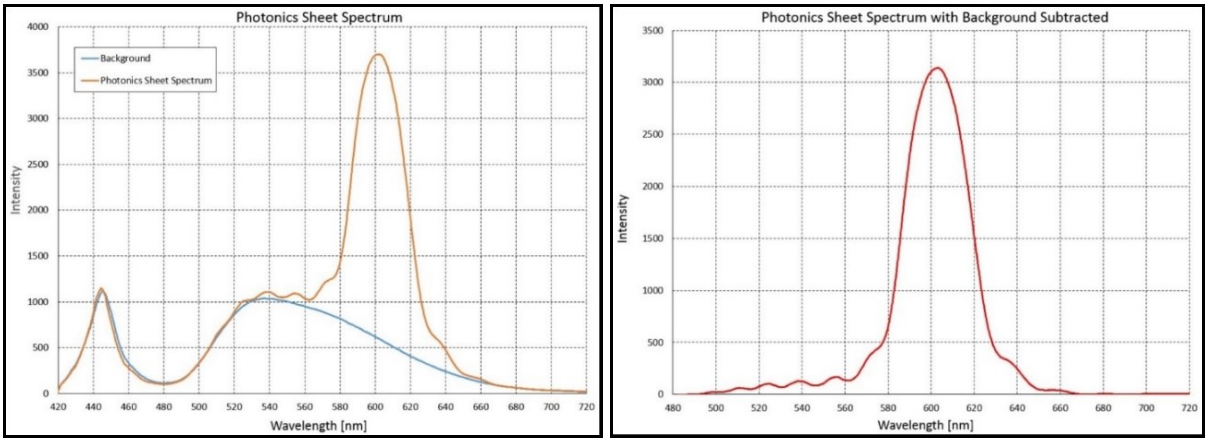

Figure 6: Raw, background, and net reflection spectrum of the opal film.

Preliminary analysis was carried out on spectra reflected from the photonic sheets to determine a reliable way of calculating the wavelength of the peak maximum. Four different methods were compared: (i) finding the channel position of the peak maximum; (ii) using

weighted average over a broad range, for example from 480 to 660 nm; (iii) using weighted average in a range of ±10 nm (i.e., ~60 channels) around the channel of the peak maximum; and (iv) parabolic (i.e., quadratic) linear and logarithmic scale fitting (in the region ±10 nm around the channel of peak maximum. All methods were tested with and without background subtraction of the normalized LED illumination spectrum. Both methods of using weighted average (within 480 to 660 nm, or ± 10 nm around the channel of the peak maximum) give consistent results and are simple enough to be implemented for determining the peak position. These methods produced reliable results, repeatability of less than ±1 channel, or less than 0.3 nm, measured on repeated spectra at the same conditions.

The initial experiments were aimed at determining the variations in the reflectivity spectra as a function of the illumination angle and observation angle of the spectrometer. The intensity increases with increasing observation angle and reaches maximum when the angle of observation is approximately equal to the angle of illumination. After that the intensity decreases, as expected for photonic crystals. The optimal illumination and observation angles were determined to be in the range 10 to 15 degree to the normal, and these angles were used for the remainder of the measurements.

The reflection spectra and peak maximum (i.e., weighted average from 490 to 660 nm without background subtraction) as a function of elongation are presented for sample VH133 in Figure 7. A predictable "smooth" behaviour of the peak maximum with respect to stretching over a wider elongation range up to 6 mm. The same type of data is presented for VH137 in Figure 8 (i.e., weighted average from 550 to 610 nm, no background subtraction). The dependence of peak maximum on the elongation for VH137 demonstrates a wavy/undulating behaviour, which was explained with sample VH137 having a thinner PET layer of 50 μm.

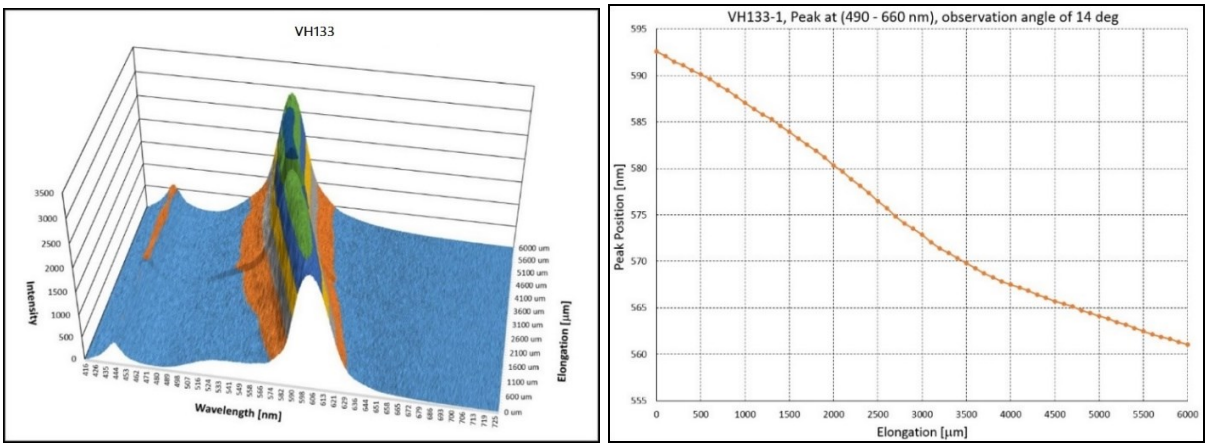

Figure 7: Reflection spectra (left) and peak position (right) versus elongation for VH133.

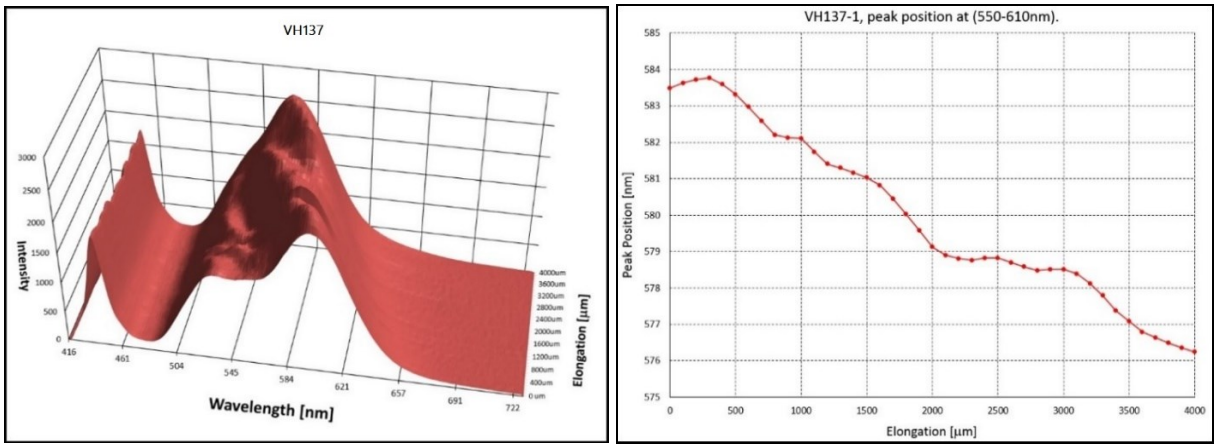

Figure 8: Reflection spectra (left) and peak position (right) versus elongation for VH137.

Elongation can be expressed as a dimensionless parameter, strain ***S***, i.e.,

$$S = \frac{L - L_0}{L_0}$$

where: L_0 is the initial length [μm], and L is the elongated length [μm], and strain S is expressed in [μm/μm], or [m/m].

The spectra presented in Figure 7 were also processed after subtracting the background. The peak position was calculated as weighted average in a range of ±10 nm around the channel of the maximum. Results are shown in Figure 9 for photonics sheet VH133. This spectral processing with background subtraction demonstrates better linearity in the range of strain up to 0.2 and gives a sensitivity coefficient of -203 nm/(μm/μm) for strains smaller than 0.2. If one assumes that it is possible to detect reliably a peak shift of 1 nm (i.e., 3 channels), the minimum detectable strain will be 0.005 μm/μm , or 0.5%. This will be sufficient for detecting changes in large cracks, or initiation of cracks, but might not be adequate for detecting small changes in the test object.

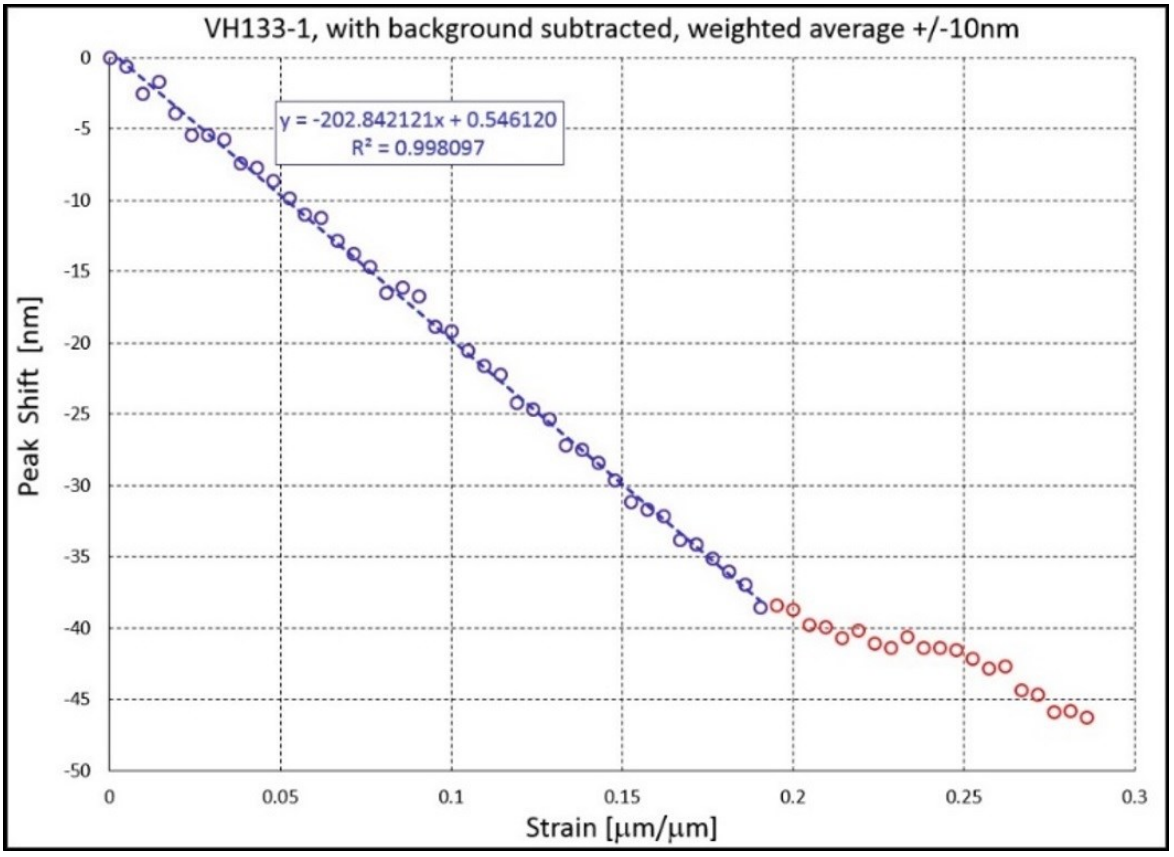

Figure 9: Sensitivity of VH133 photonic sheet to strain (with background subtraction).

It is important to note that what essentially is tested in the stretching experiments are the properties of the combined system of the substrate and the opal film. As far as the thickness of the opal film is substantially smaller than the thickness of the substrate, for a free-standing sample we are testing the elastic properties of the substrate.

After the samples were stretched to maximum elongation, between 4 and 6 mm, the sample elongation was reduced gradually until the sample started bending, which happened between remaining elongation of 2 to 3 mm. Based on this observation, the relaxation length (i.e., the elasticity region, before sample starts bending) was assumed to be more than 1 mm.

3.2 Cyclic stretching

Strips from samples D100-18, D100-19, D100-22, D100-23 and D100-24 were used to characterize the dependence of the spectral reflectivity on elongation during multiple cyclic stretches of photonics sheets. A strip of each sample was clamped between two micrometer stages and stretched at steps of 100 µm up to 1 mm (referred to as a forward stretch in the figures). From a stretch of 1 mm, the sample elongation was reduced with the same steps of 100 µm back to the initial zero position. This was repeated two to four times. At each step, a spectrum of the photonics sheet was measured, and the position of the peak was determined as weighted average over region 540 to 630 nm. For some of the samples, when returning to zero elongation, for the last positions of 300 to 100 µm, the strips started bending, indicating loss of elasticity. Also, a slow creep (i.e., changes in the reflected spectra with time) was observed within a minute of setting some of the stretch positions. For some of the samples, the loss of elasticity was consistent. Similar behaviour was observed for all tested samples. Results for D100-18 and D100-19 are presented in Figure 10. Forward and backward scans are grouped separately, which is a clear indication of a hysteresis effect. Again, what is evaluated in such experiments is mainly the elastic properties of the substrate, so the observed hysteresis effect is associated with the substrate, and not with just the opal film. Good repeatability was observed, indicating the possibility to use photonic sheets on samples where cyclic stretching is expected.

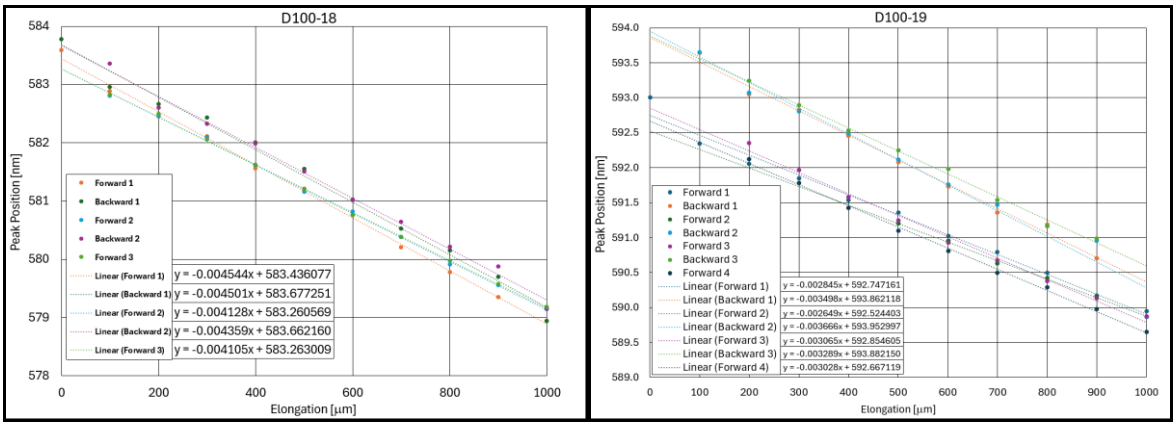

Figure 10: Peak position versus elongation during cyclic stretching.

3.3 Heating and loading of concrete block

The aim of the next test was to evaluate the response of the photonic sheets attached to a concrete block during heating and loading. The setup for the heating and loading experiment is shown in Figure 11. Photonics sheets were glued on top of cracks which had been previously identified using Digital Image Correlation (DIC) on the same block for similar temperature ramp, shown in Figure 12. The first test was a stability tests performed for ~4 hours at room temperature (~26ºC). During the next test, the cavity in the centre of the concrete block was filled with water and was heated with an electrical heater for approximately 8 hours. During this time, the concrete surface temperature, measured close to the location of the photonics sheet, changed from 22.8ºC to 35.8ºC. The results are shown in Figure 13. Based on the performed measurement, it is possible to associate the thermal expansion of a combined photonic sheet, concrete surface, and glue affixing the sheets, with the observed peak shift. One can also speculate that the photonics layers (opal film) swell

with temperature, thus increasing the distance between the colloidal crystal planes, and hence there is a “red” shift in peak position (i.e., an increase of the peak wavelength).

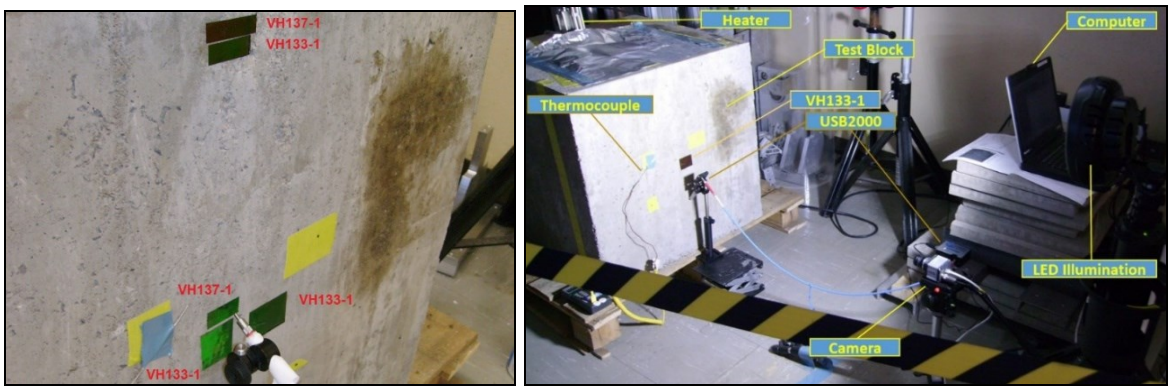

Figure 11: Experimental setup for concrete block during heating and loading.

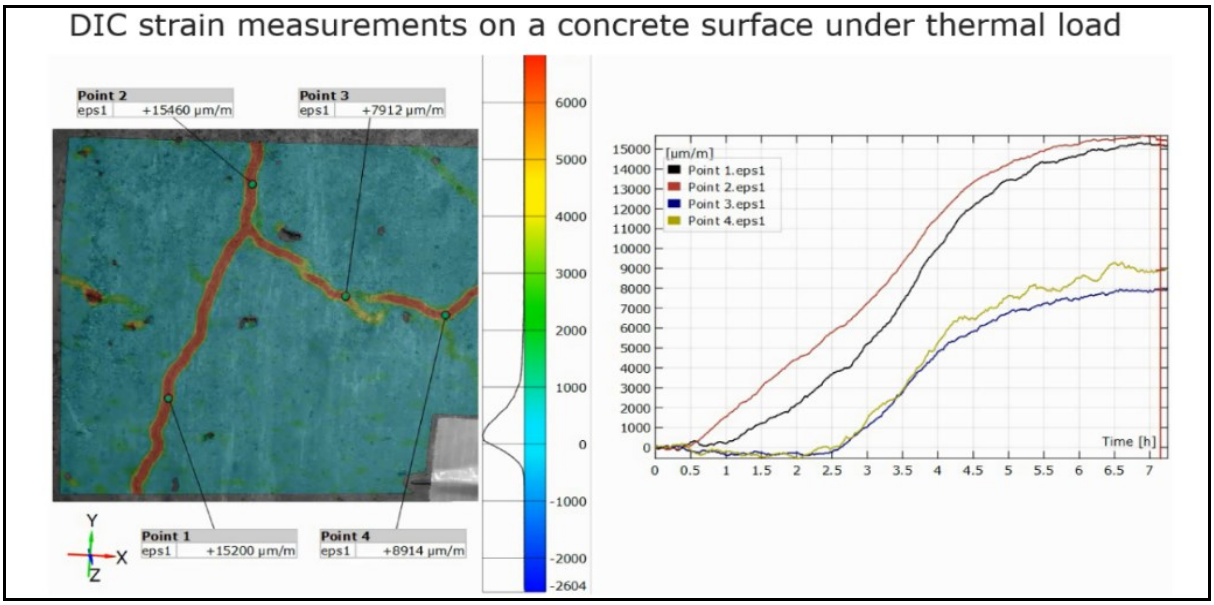

Figure 12: DIC measurements of the same area where photonics sheets were placed.

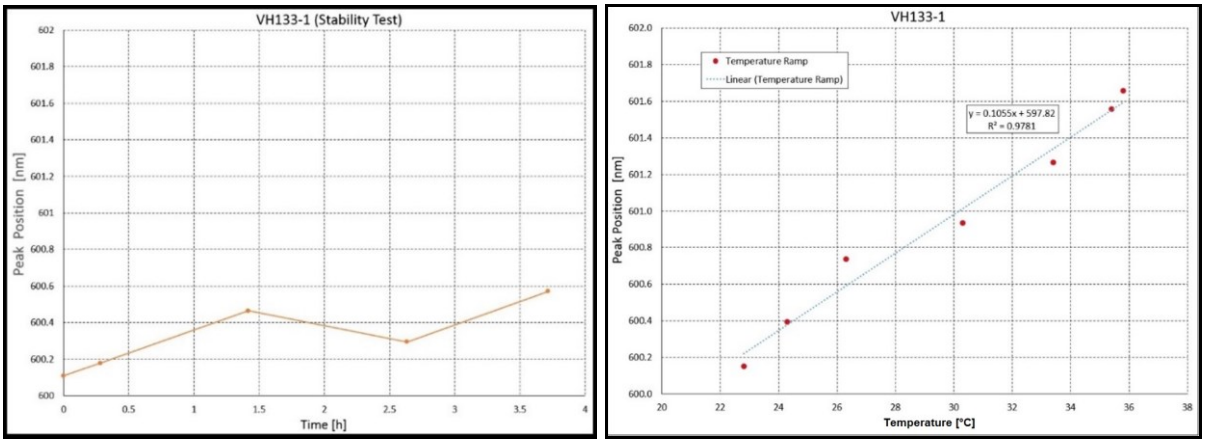

(a) Stability Test (b) Temperature Ramp

Figure 13: Peak position vs. time during stability test (a) and temperature ramp (b).

In the next test, the same concrete block was used, and stress was applied from inside the cavity using two 2-ton jacks. The purpose of the experiment was to attempt to simulate the expansion of a reactor containment structure during the pressurization when leak testing a building. Pressure was applied in two directions: (i) parallel to the surface of the photonics sheets, and (ii) perpendicular to the surface of the photonics sheets. The pressure was increased in four steps, and then released. Several reflection spectra from the photonics sheets were recorded at each of the four steps. The standard processing of the spectra was used, i.e., subtracting a normalized background and determining the peak position as weighted average in the region 580 to 625 nm. The results are shown in Figure 14. For the parallel expansion, the four increasing pressure steps and the release of pressure are identifiable in the plot. For the perpendicular expansion, practically no peak shift was observed. At most of the pressure increase steps, a relaxation effect was observed with time. With the amount of applied force, the overall effect, i.e., the peak shift, is smaller than that for the temperature effect.

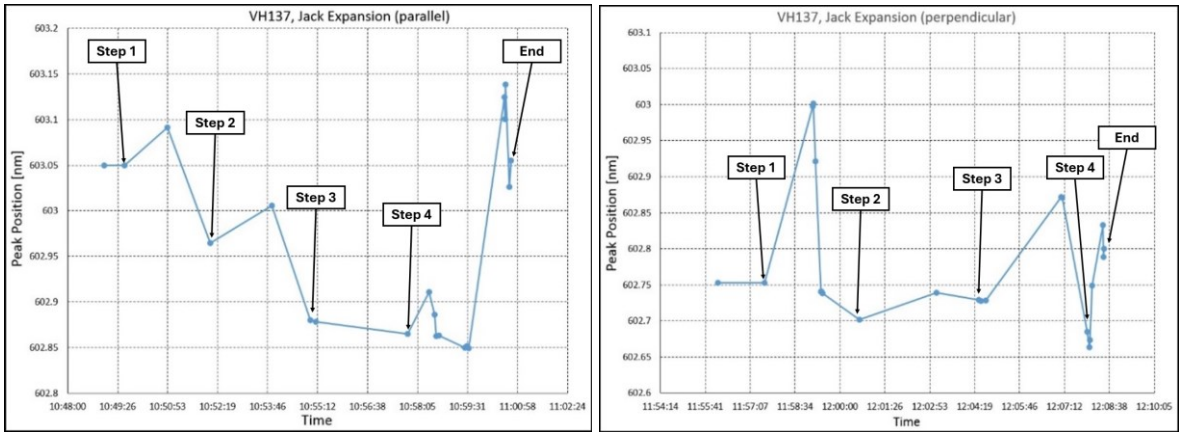

(a) Parallel jack expansion test (b) Perpendicular jack expansion test

Figure 14: Results from the jack expansion test.

3.4 Stand-off monitoring with camera

Stretching experiments were performed as per the setup shown in Figure 4, using images recorded with a high-resolution 10 megapixels colour camera from IDS Imaging Inc. Both a high brightness LED panel and ambient fluorescent room lighting were used for illumination (as shown in Figure 2). The colour camera Red/Green/Blue (RGB) settings were adjusted for the R, G and B histograms to overlap on neutral grey sample. This served as a reference for measuring the RGB shift on the photonics sheets as they were stretched. Separate set of strips from samples D100-18 and D100-22 were elongated to 5 mm with 200 μm steps, and images of the strips were recorded at each step. During the forward stretch, a white LED illumination was used. After completing the forward stretch, the elongation of the sample strips was reduced with the same step (i.e., 200 μm) backwards under the ambient fluorescent illumination, until the sample lost elasticity and started to bend. For both samples the backward scan was stopped at ~3 mm elongation. The RGB colour images were used to extract the R, G, and B components, for which the averaged values were calculated over the areas of interest.

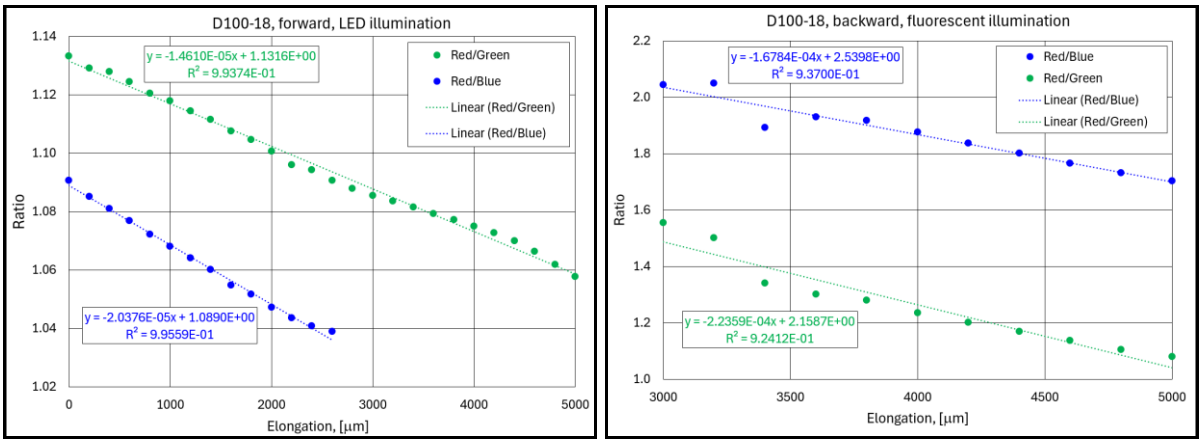

Figure 15: Linear fit of RGB ratios vs elongation for D100-18.

The ratios R/G (red/green) and R/B (red/blue) are plotted as a function of the elongation in Figure 15 for sample D100-18. The linear fits for the forward stretch (LED illumination) and for the backward direction (fluorescent illumination) are presented in the same Figure. For the forward stretch (i.e., LED illumination), linear dependence of the R/G ratio vs elongation was observed up to 5 mm stretch, while R/B ratio demonstrated linear dependence on the stretch up to 2.5 mm. For the backward direction, with fluorescent illumination, the elongation range was from 3 to 5 mm, and both ratios R/G and R/B demonstrate linear dependence on elongation over the whole region. Fluorescent illumination led to bigger sensitivity coefficients for R/G and R/B, in the order of 10^{-4}, when compared to LED illumination, with sensitivity coefficients in the order of 10^{-5}. Based on the presented results, it is possible to conclude that the method of using high-resolution colour camera followed by calculation of the R/G and R/B ratios can be used for qualitative and quantitative assessment of the elongation/strain, despite the fact that the linear proportionality coefficients are relatively low.

4. Conclusions

This paper presents experiments with opal photonic crystal films, aimed at evaluating their properties and the possible approaches for using these devices for NDT. The strain visualising and measuring capabilities of the photonic sheets were demonstrated. Photonic sheet reflection spectra are sensitive to both observation angle and elongation, that is, both sample elongation and change of the observation angle can lead to the same results. In order to address this issue, a compact handheld holder was manufactured, which housed the illumination LED and the fibre-optic tip of the spectrometer at a fixed angle of illumination and observation. Four types of spectrum processing were evaluated for determining peak position of the reflection peak. The "strain sensitivity" of the photonic sheets was studied with a fibre optic spectrometer, and a linear response sensitivity coefficient of ~ -200 [nm/(µm/µm)] of the strain versus peak shift was observed up to strain of 0.2 [µm/µm]. It was concluded that an elongation in the order of 0.5 mm is needed for reliably observing colour changes (peak shift) with a spectrometer or with a high-resolution colour camera.

Additional experiments were performed with the photonic sheets attached to concrete block. Two types of loads were used: heating of the concrete block and applying pressure using jacks. A linear dependence of the reflection peak position with temperature was observed, while no dependence was observed when applying pressure using jacks. Some of the photonic sheets strips were placed (glued) over known cracks, but the crack expansion/change due to the used loads was too small to be observed with the photonic sheets.

One of the advantages of the photonic sheets is that they can be observed from a distance, i.e., they can be used in difficult to access placed. A technique for stand-off non-contact measurement of photonic sheets with colour camera was developed, and a methodology for processing the images was proposed. Linear dependence of the ratios of the RGB components on the elongation of the photonic sheets was observed.

Next steps in the stand-off measurement of photonic sheets will be to evaluate the use of multi-spectral cameras and polarization cameras for determining the elongation of the photonic sheets and corresponding strain.

The overall conclusion is that the opal photonic crystal films can be used as low-cost NDT tools for visualisation and measurement of deformation and strains.

References

1. H. Fudouzi, "Fabricating high-quality opal films with uniform structure over a large area", Journal of Colloid and Interface Science, Volume 275, Issue 1, 1 July 2004, Pages 277-283
2. H. Fudouzi and T. Sawada, "Photonic Rubber Sheets with Tunable Color by Elastic Deformation", Langmuir, v. 22 (2006), p. 1365-1368
3. Hiroshi Fudouzi, "Tunable structural color in organisms and photonic materials for design of bioinspired materials", Sci. Technol. Adv. Mater., v. 12 (2011), p. 064704
4. H. Fudouzi, T. Sawada, Y. Tanaka, I. Ario, T. Hyakutake, I. Nishizaki, “Smart photonic coating as a new visualization technique of strain deformation of metal plates”, Proceedings of SPIE, v. 8345, p. 83451S-1, presented at “Sensors and Smart Structures Technologies for Civil, Mechanical, and Aerospace Systems 2012”
5. H. Fudouzi, K. Tsuchiya, S. Todoroki, T. Hyakutake, H. Nitta, I. Nishizaki, Y. Tanaka, T. Ohya, “Smart photonic coating for civil engineering field: for a future inspection technology on concrete bridge”, Proceedings of SPIE, v. 10168, p. 1016820, presented at “Sensors and Smart Structures Technologies for Civil, Mechanical, and Aerospace Systems 2017”
6. Z. Yang, M. Koyama, H. Fudouzi, T. Hojo, and E. Akiyama, "Availability of opal photonic crystal films for visualizing heterogeneous strain evolution in steels: example of Lüders deformation", ISIJ international, vol. 60 (2020), no. 11, pp. 2604–2608
7. Y. Tanaka, H. Fudouzi, and T. Hyakutake, "Feasibility study of visualizing strain distributions using opal film", ISIJ international, vol. 62 (2022), no. 1, pp. 257–262
8. Y. Zhou, Z. Yang, M. Koyama, S. Ajito, T. Hojo, H. Fudouzi, E. Akiyama, "Quantitative Evaluation of the Relationship between Strain and Color Change in Opal Photonic Crystal Films and Application into Complex Specimen Geometries", ISIJ International, Vol. 62 (2022), No. 10, pp. 2061–2068